Development of a Low-cost Flutter Test Bed with an EPS Foam Model for Preliminary Wing Design

Abstract

This paper discusses a novel, low-cost approach for the design and testing of a flutter test article made out of expanded polystyrene (EPS) foam. In the present study, this set-up was used as a precursor to testing a highly flexible, inflatable wing, but could just as easily be used in the flutter testing of any structure with complex shape and mechanical properties. The material properties of EPS foam were tested using two different approaches: a 3-point bending test based on ASTM Standards for cellular materials and a new finite element model updating approach that used experimental data collected from simple ground vibration tests (GVT). It was found that the second approach provided material properties that were the most representative of the behavior of the specimen under flutter loads. That information was then used in a computational aeroelastic flutter model of the EPS foam wing. Wind tunnel flutter tests were performed for the EPS foam model. The computational frequency domain decomposition (CFDD) method was used to identify modal parameters and the damping trend extrapolating method was used to predict the critical flutter speed from pre-flutter experimental data. The flutter results from this aeroelastic model were in good agreement with the test data.

Keywords: Low-cost flutter testing, Wind tunnel test, EPS foam, Flexible wing

Nomenclature

C_L	=	Lift coefficient
E, G	=	Young's modulus and Shear modulus of EPS foam

f_n	=	Peak resonance frequency
f_{lb},f_{ub}	=	Lower and upper bound frequency at $\frac{\text{peak amplitude}}{\sqrt{2}}$
g	=	Structural damping
ζ	=	Damping ratio
ACF	=	Aerodynamic Correction Factor
AoA	=	Angle of Attack, degrees
DIC	=	digital image correlation
EPS	=	expanded polystyrene foam
FMP	=	Flutter margin parameter
GVT	=	Ground Vibration Test
WB1	=	First Wing Bending Mode
WB2	=	Second Wing Bending Mode
WIB1	=	First Wing In-plane Mode
WT1	=	First Wing Torsion Mode

1. Introduction

Understanding flutter behavior is an important requirement for the reliable flutter speed prediction of future innovative air vehicle designs, especially for those with high aspect-ratio, flexible wings. Classical flutter is a dynamic instability problem that occurs due to the aeroelastic coupling between the bending and torsional structural modes caused by the interaction of structural and aerodynamic forces [6]. As airspeed approaches the flutter speed, the structure begins to absorb energy from the flow, leading to oscillations with increasing amplitudes until sudden structural failure or limit cycle oscillations due to wing non-linearities occur. Frequency domain based numerical flutter prediction methods, such as the $p-k$ method, are used to obtain the complex eigenvalues of the dynamic system to

predict this instability. The flutter speed is computed by identifying the velocity at which the damping component of the complex eigenvalue becomes a positive value[12].

This paper presents a numerical and experimental flutter analysis of an expanded polystyrene (EPS) foam wing model. Here, the study explored the complexities introduced into the flutter analysis due to nonlinear material behavior and suitable mitigation strategies to extract meaningful inferences from these results. Whereas there exists a vast amount of literature on flutter analysis in both the numerical and experimental domains, discussion on low-cost, easily reproducible strategies that can be used as a test-bed for more complex structures is limited. Such a step is important as flutter testing is expensive and time-consuming and can often have additional constraints placed on the testing timeline in the form of availability of sophisticated testing facilities like a full-scale wind tunnel. Due to the unavailability of literature discussing mitigation strategies such as the development of test beds, much of the preliminary stages of flutter testing are often spent on trial and error steps performed on models that can be expensive and time-consuming to fabricate. This gap is addressed herein by presenting a detailed report of flutter analysis and verification methods using an easy-to-fabricate foam wing model to represent very flexible wings.

This work was motivated by the authors' interest in studying kite-like air vehicles with inflatable wings, where aeroelasticity was identified as one of the areas of concern due to the flexibility and the large aspect ratio of the wing [25]. The fabrication of real inflatable wing models comprise of an intricate process involving precision cutting of the fabric, alignment and bonding by impulse heat sealing, and required many man-hours [18]. The advantage of having a low-cost test bed at the preliminary stages of testing are discussed in this paper by comparing it with the full-scale testing of this inflatable wing. But it must be noted that any complicated flutter testing model, having complex geometries, material properties or dynamic behavior, could benefit from this precursor step.

EPS foam was chosen as it can be used to create a light weight structure, having the

same shape as the inflatable wing. It can be easily shaped into models with the required outer mold-lines. The material is also cost effective and, therefore it is suitable for fabricating multiple models in the experiment design process, while ensuring that they were exact duplicates of each other in shape. In the present work, EPS foam also afforded some insight into the effect of material nonlinearity in the context of flutter testing. At the same time, it provided a firm enough test bed to check the flutter testing equipment in the preliminary stages of the experimental design. The ease of instrumentation also came from the ability to cut and embed electronics and connectors without the use of sophisticated equipment. This step enabled the testing and verification of the sensors without the added complications of compressors and pressure gauges needed for an inflatable wing. For the same reasons, this also provided a suitable test bed to perform mass balancing and developing an understanding about how the mass distribution affected the flutter frequencies and modes.

Another advantage is that the models can be created at very different scales according to the needs of the preliminary tests. For example, where the availability of a full-scale wind tunnel is limited, it is possible to conducted a scaled down version of the test in an open-jet wind tunnel as the first step. However, it is very difficult to fabricate an inflatable wing at small scales due to the nature of the manufacturing process. Low cost test-beds are crucial in this case to allow experimentalists to perform trial and error steps that still yield reasonable insights into the full-scale, resource-intensive test that they are yet to perform.

One of the important considerations in flutter prediction is the damping coefficient that must be used in the calculations. The two important types of damping are classical viscous damping and structural damping. In classical damping, the damping force is proportional to the velocity. Structural damping is used to quantify the internal material damping as well as the damping caused by features such as rivets and joints and free-play present in the structure. This type of damping is assumed to be proportional to the displacement, but it acts in the direction opposite to the velocity, i.e. it lags the displacement by 90 deg. The

Federal Aviation Administration provides a conservative value of 3% structural damping for metals [1]. Owing to the higher energy absorption quality of porous, cellular materials such as EPS foam, a higher damping of 5% was used in this work. This value was obtained by scaling the damping coefficient used by Ozturk and Anlas in [17] with respect to the ratio of the density of the foam in this study and the density of the EPS foam used by them. This was considered a reasonable approximation as it has been shown that density is an important parameter in determining the energy absorption characteristic of EPS foam [20].

This study was carried out in two parts: 1) determination of material properties of the EPS foam and corroborating the response of the test article at expected excitation frequencies, and 2) experimental flutter testing and verification against the numerical model developed in the previous step. Details of some observed discrepancies between the supplier-given ESP foam material properties and observed vibration response of the model are discussed. This led to a comparative study between an iterative model updating procedure and ASTM-based experimental material testing. The finite element model updating technique developed for this work is discussed by Zhao et al. [24]. Standard ground vibration tests (GVT) were carried out to extract the experimental data needed for this procedure.

A number of methods are available in the literature to identify the flutter mode from tests, namely extrapolating damping trends, the envelope function approach, the Zimmerman–Weissenburger flutter margin, and discrete-time auto-regressive moving-average (ARMA) model [13]. The computational frequency domain decomposition (CFDD) method was used to obtain modal parameters with output-only data [11]. This method is based on the peak-picking approach and curve fitting of the cross power spectral density diagram. For well-separated modes, this technique gives an acceptable estimate of the modal parameters, including modal frequencies and modal damping ratios [19]. The most common data-based method for flutter prediction is the method of extrapolating damping trends. This predicts the onset of flutter mode by extrapolating the trends of the modal damping with varying

wind tunnel air speeds [23]. Based on a previous study performed by the authors on the flutter of a thin, flat metal plate model in the same test setup [15], the extrapolating damping trend method was chosen as the method to estimate the flutter speed.

Techniques like modal filtering and modal parameter estimation are required as aeroelastic wind tunnel data usually has a low signal to noise ratio (SNR) [22]. The noise in the signal arises from multiple sources such as unknown turbulence input, wind tunnel fan noise and instrument noise. The extrapolating damping trends method approach uses data obtained at various wind tunnel air speeds lower than the expected flutter speed to obtain the damping ratios as a function of air speed. This allows one to predict the actual onset of the flutter mode through extrapolation to the air speed where damping becomes zero or a prescribed small positive value.

The main objective of the tests studied in the present work was to verify the flutter speed identification methods and structural and aeroelastic numerical models that were developed for the flutter speed computation of a structure with material non-linearity. In addition, the numerical models were used to verify the in-house code that was developed for the aeroelastic analysis of a high aspect-ratio inflatable wing [25]. The remainder of the paper is organized as follows: Section 2 presents the design of the EPS foam flutter test article. The material properties of the EPS foam were obtained from both three-point bending tests following ASTM C203 and C393 guidelines and model updating based on ground vibration tests. Section 3 presents the flutter test setup, flutter speed identification strategy and the results. The last section, Section 4, summarizes the overall findings of this study.

2. Foam Wing Model

This section describes the numerical modelling, testing and analysis performed on the test article. The airfoil shape was chosen to represent the outer mold line of a future inflatable wing [25].

2.1. Model Details

The airfoil of the EPS foam model was generated to be representative of an inflatable wing with a 20% reduced thickness NACA 4318 airfoil, inflated at a 1.72×10^4 Pa (2.5 psi) net internal air pressure and having eight baffles (see Fig. 1). The actual inflatable wing airfoil shape would be covered by a thin film as shown in Fig. 1 to improve aerodynamic performance of the fully inflated form.

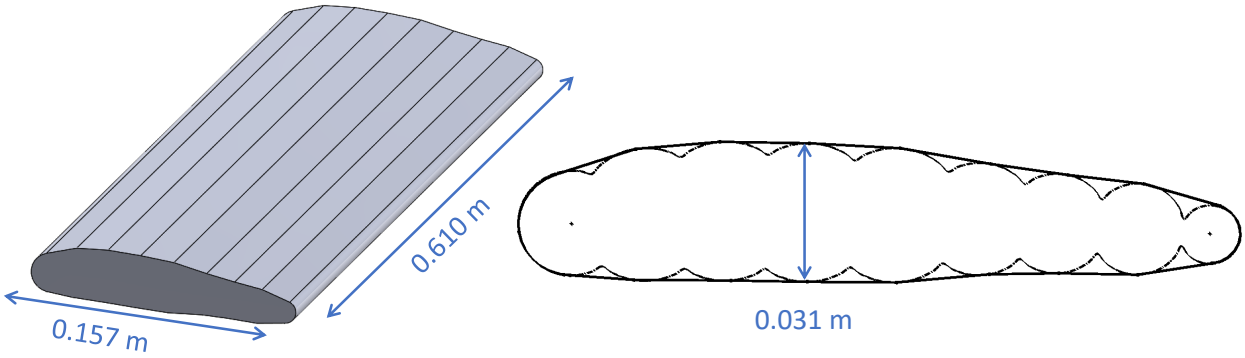

Figure 1: CAD model of the foam wing flutter test article

The model was developed with experimental verification in mind. Thus, the span and chord of the foam model were chosen to be 0.610 m (24 in) and 0.157 m (6.18 in), respectively, to satisfy the size requirements of the open-jet wind tunnel available at Virginia Tech. Ballast masses were placed at 86.4% chord as shown in Fig. 2 to reduce the flutter speed, increasing the chances of it falling within the testing speed envelop of the wind-tunnel. The reasoning behind this is that the increase in the mass moments of inertia of the model with the addition of the ballast masses would result in the reduction of the flutter speed [12]. The use of EPS foam for the small-scale wind tunnel model facilitated this approach.

2.2. Determination of EPS Foam Material Properties

The determination of the mechanical properties of EPS foam is quite involved compared to uniform material like aluminum. The Young's modulus and the shear modulus depend on the density of the foam. As EPS foam is a cellular material with trapped air pockets it is is

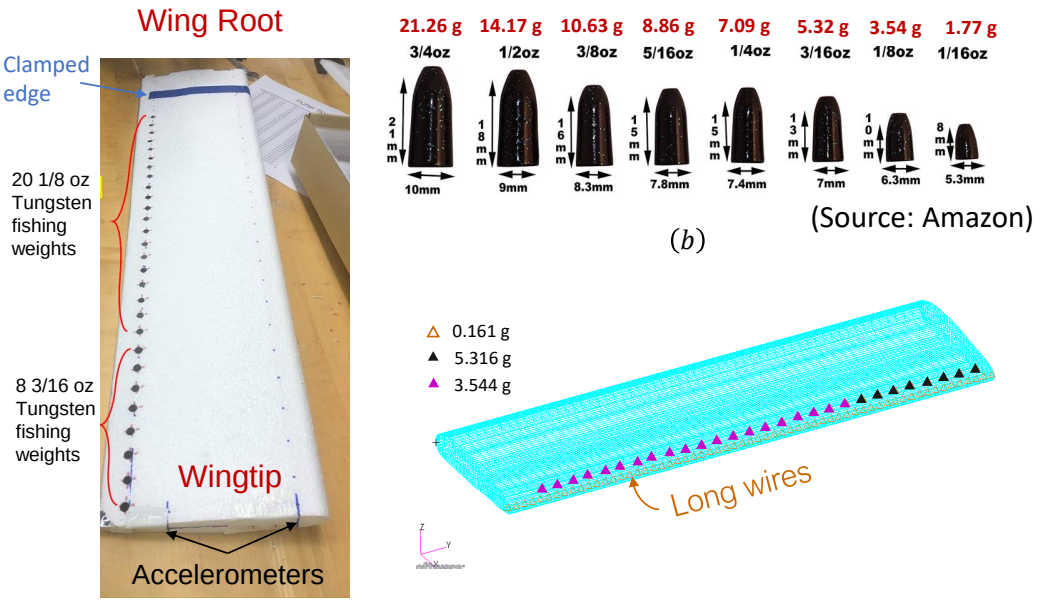

Figure 2: (a) Foam Model Test Article, (b) Tungsten Weight and (c) Finite Element Model

difficult to ensure the same mechanical behavior for two different samples. Because of this, material testing standards like those provided by ASTM, provide different approaches for different applications of cellular plastic, such as packaging, geofoam and insulating material.

In addition to density, the mechanical properties heavily depend on the strain rate under dynamic loads. When compressive forces are applied the entrapped air starts to generate increasingly higher viscous forces, which in turn leads to increased sensitivity to the strain rate [16, 9, 14]. This is of particular interest to the present study as the flutter test involved testing the wing specimen at increasing air speeds that, i.e. increasing strain rates.

The shear modulus of cellular foams is even more difficult to determine accurately via tests than Young's modulus. It has been demonstrated that the shear modulus depends on the thickness of the specimens used in the tests [5]. It is also hard to ensure proper boundary conditions and perform shear tests such as for uniform materials like metals. Here too, standard material tests are provided with specific applications in mind. Hence the values determined through such methods might not be applicable under different loading

conditions.

From the literature it is clear that the EPS foam material properties that are used in the numerical model should be determined in a manner specific to this application. As such, two material testing approaches were examined and compared, the first one being the conventional static three-point bending test approach, and the other, the estimation of the properties via a simple ground vibration test that simulates the strain rates the material experiences during flutter.

2.2.1. Approach 1: ASTM-based Material Testing

ASTM-based material tests were carried out to determine material properties of the EPS foam used in the model. For this purpose, standard rectangular samples of foam of density 1.0 pcf were obtained from the same manufacturer as the airfoil models. For the elastic modulus (E), a three-point bending test was carried out as per ASTM C203-05 [3], using the standard universal testing (UT) machine shown in Fig. 3(a). A three-point bending fixture with cylindrical bearing surfaces (as recommended in ASTM C203-05) was used. This is shown in Fig. 4(a). Figure 4 shows the dimensions of the standard rectangular specimens used in the material testing. Mid-point deflection D, obtained from the cross-head movement at a given load P was used to calculate the Young's Modulus as in Eq. 1 [3]. With respect to the bending direction here, the second moment of inertia, I, is given by $wt^3/12$. Five samples of cross-sectional dimensions 30.5 cm $\times$ 10.2 cm $\times$2.5 cm (12 in $\times$ 4 in $\times$ 1 in) ($L \times w \times t$) were tested at a span $h = 25.4$ cm (10 in), and the average E was calculated.

$$E = \frac{PL^3}{48ID} \tag{1}$$

The determination of the shear modulus (G) proved to be more challenging. After some preliminary studies, it was decided to use sandwich beam samples, having steel shim stock

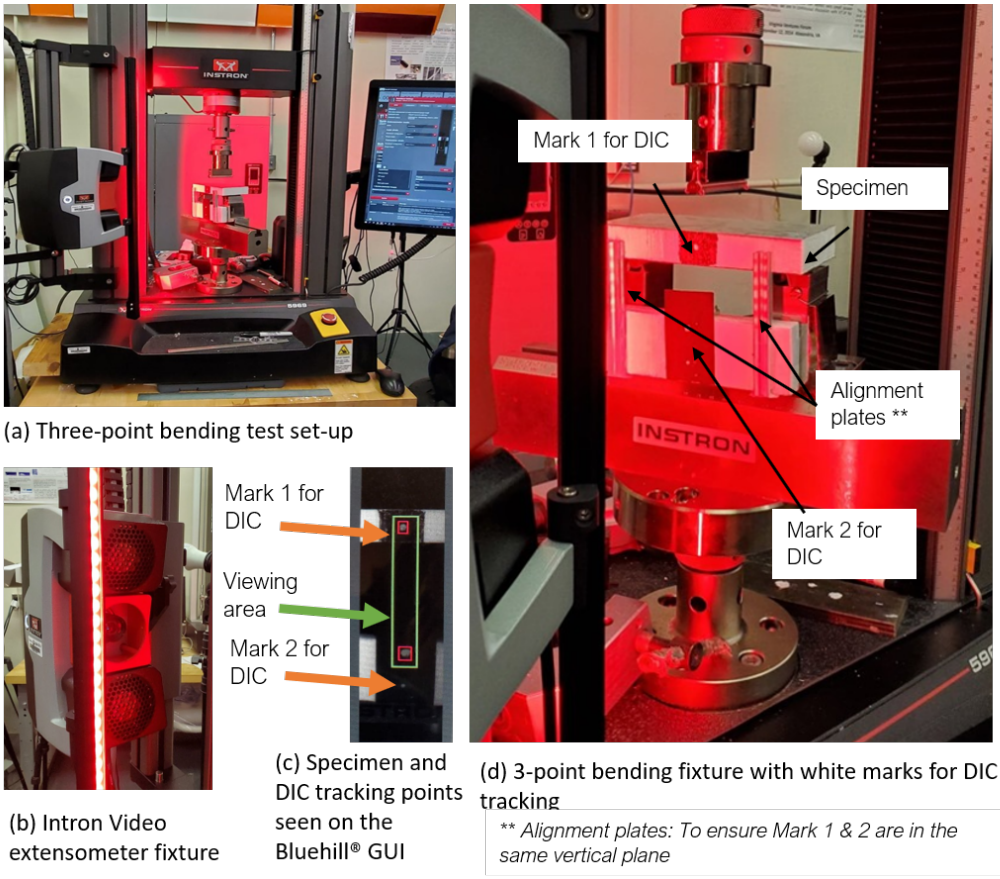

Figure 3: Set-up for ASTM Material Testing

facings and a foam core. The facing sheets placed on either side of the foam core helped restrain local, uncontrollable deformations of the foam sample to some extent. Steel was chosen due to its availability in very thin plates (thickness of 0.076 mm (0.003 in) was used here). This ensured that the major contribution of the shear component in the midpoint deflection came from the foam, not the steel facing. In addition, owing to the high level of quality-control and homogeneity possible in steel manufacturing, reliable material properties were readily available. So, its contribution to the observed deflections can be calculated with suitable accuracy. The facing and the foam core were bonded together using epoxy glue.

The testing procedure specified in ASTM C393/C393-M-16 [2] was used, together with digital image correlation (DIC) for non-contact mid-point deflection measurement. Figure 3 shows the complete set-up used for the foam shear modulus determination. An in-built mark-

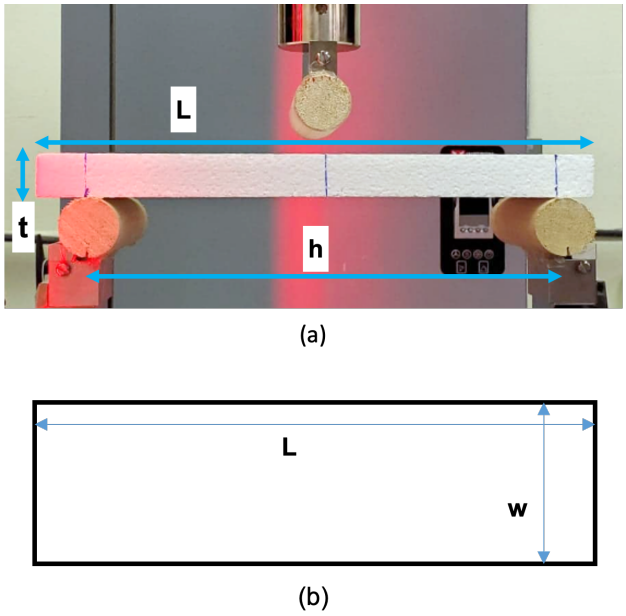

Figure 4: (a) 3-point bending test set-up, (b) Rectangular EPS foam specimen (Planform)

tracking DIC capability of the UT system and the video extensometer fixture (Fig. 3(b)) were used for this purpose. The shear modulus was found to be very sensitive to the displacement measurements. So, using cross-head motion to measure the sample mid-point deflections was not feasible due to the presence of local deformations of the sample at the point of load application. Five specimens of cross-sectional dimensions 15.2 cm × 8.9 cm × 2.5 cm (6 in × 3.5 in × 1 in) were tested at a span of $h = 10.2$ cm (4 in), and the average of the values of G from each test was computed.

2.2.2. Approach 2: Ground Vibration Test

The material properties of EPS foam were also found via an iterative model updating procedure that determined the best fit between the data collected from a ground vibration test (GVT) and a finite element (FE) model. This involved the comparison of modal frequencies, damping and mode shapes from both models. A description of the test setup, model updating step and the vibration test results are presented next.

Test Setup

The foam model described in Section 2 was fabricated using EPS foam and mounted in an upright position as shown in Fig. 5. It was attached to an immovable support by first fixing it to a 3D printed base and then clamping the base to a supporting structure such as a heavy laboratory workbench. The 3D printed base was specially manufactured with a slot of the same shape as the outer mold line of the wing model. The wing model was inserted into this slot and was firmly glued to the base along the contact surface. This minimized any damage to the wing model during the assembly process while ensuring a fully clamped boundary condition at the wing root.

The ground vibration test was conducted using the laser vibrometer setup shown in Fig. 5. Base excitation was applied by a shaker, and the resulting displacement of the wing model was captured by a laser vibrometer. A LDS V203 shaker was located near the wing clamped edge as seen in Fig. 5, and the excitation was applied via a steel stinger connected to the shaker and touching the model. The sensitivity of the load cell for the shaker was 512 mV/lbf, and the VD-02 Decoder from the laser scanner was 25 mm/s/V. The data was recorded at 2 kHz sample rate, well above the 55 Hz which is the maximum frequency of interest. A grid of 7×3 light-weight reflective tape markers were placed on the foam model to enhance the quality of the reflected laser beam without causing any significant change to the structural properties of the wing. These markers were later removed in the wind tunnel test discussed in Section 3 as they might influence the aerodynamics by altering the surface of the model. The test was repeated by directing the vibrometer at each grid so that the mode shapes could be evaluated covering the 2D surface of the wing model.

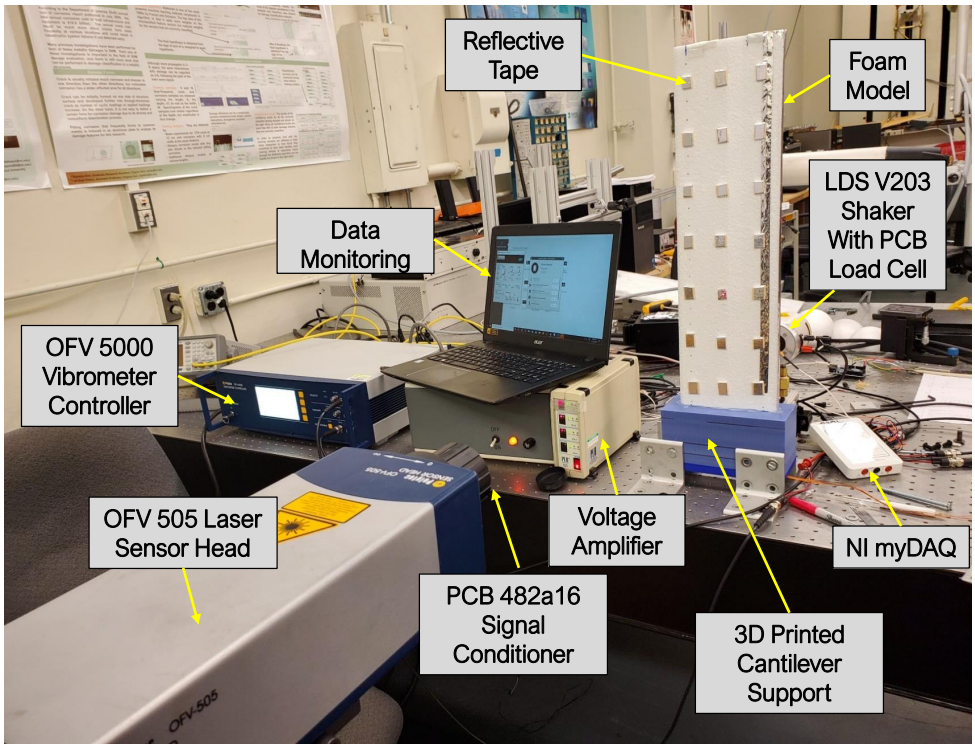

Figure 5: Ground Vibration Test of Clamped Foam Wing Model

Numerical FEM Model

A NASTRAN finite element model was developed for this foam wing. The EPS foam was modelled as an isotropic material similar to that used by Ozturk and Anlas [17]. A high-fidelity FE model was created using 8-noded hexahedral solid elements. A mesh of 19,740 elements was required for converged results of vibration and flutter analysis (the latter is discussed in Section 3).

The effect of the mass of air surrounding the wing, called the *added-mass effect*, must be considered when the wing structural mass is comparable to the mass of the surrounding air. This added-mass effect should be considered in both vibration and flutter analysis [10, 21]. Brennen [7] has summarized the added mass effect for various body shapes. For the foam wing used in the present study, the surrounding air was modelled through the 6×6 mass matrix model given in Eq. 2 [10, 21].

$$\boldsymbol{m}_{add} = \begin{bmatrix} k_{trans}\dfrac{\pi\rho t^2 b}{4} & 0 & 0 & 0 & 0 & 0 \\ 0 & k_{trans}\dfrac{\pi\rho t^2 c}{4} & 0 & 0 & 0 & 0 \\ 0 & 0 & k_{trans}\dfrac{\pi\rho c^2 b}{4} & 0 & 0 & 0 \\ 0 & 0 & 0 & k_{rot}\dfrac{\pi\rho c^2 b^3}{48} & 0 & 0 \\ 0 & 0 & 0 & 0 & k_{rot}\dfrac{\pi\rho b^2 c^3}{48} & 0 \\ 0 & 0 & 0 & 0 & 0 & 0 \end{bmatrix} \tag{2}$$

where c, b and t are the chord, the span and the thickness of the wing, respectively; k_{trans} and k_{rot} are factors accounting for the 3D effects that occur due to the foam's finite length, depending on wing aspect ratio, whose values can be found in [21].

The length of the foam-only model was measured to be 0.554 m (21.8 in), with a chord of length $c = 0.157$ m (6.18 in), a cross section area $A_w = 3.922 \times 10^{-3}$ m^2 (6.08 in^2), and the material density of $\rho_W = 12.29$ kg/m^3 (0.77 pcf). The total mass was measured to be 2.940×10^{-2} kg (0.0648 lbs). The structure to fluid mass ratio was 0.52. Here, the mass ratio is defined as $\rho_W A_w / \pi \rho_f c^2$ for the air density ρ_f of 1.204 kg/m^3 (0.075 pcf). The foam density obtained using the wing model was used in the finite element model. The mass of the finite element model was close to the measured mass of the full model including ballast masses as seen in Table 1. In addition, the mass distribution of practical components like the connecting wires for accelerometers (shown in Fig. 2(c)) were also accounted for, which results in a slightly larger mass than the calculated mass of the wing model alone.

Table 1: Mass Comparison of the Foam Model including Ballast Mass

Measured mass (kg)	FEA mass (kg)	Diff.
0.153 (0.337 lbs)	0.149 (0.329 lbs)	-2.373%

Table 2 shows the identified vibration mode results obtained from ground vibration test.

The finite element analysis vibration mode frequencies using the material properties for the EPS foam provided by the supplier (see Table 3) are found to be lower than the test results. A finite element model updating was conducted in an iterative manner to match the mode results by updating the material properties [24]. The modal frequencies of the final finite element model with the updated material properties matched well with test results as seen in Table 2. The free vibration mode shapes for the foam model with updated material properties are compared against the three identified mode shapes, and they are found to be in a good agreement as seen in Fig. 6.

Table 2: Modal Results of Present Foam Wing with Ballast Masses

Mode shapes	Test data (Hz)	Initial FEM (Hz)	Updated FEM (Hz)	Diff.
First bending mode (WB1)	4.10	2.13	4.15	1.22%
First inplane bending mode	N/A	9.97	20.58	N/A
Second bending mode (WB2)	26.30	14.31	23.87	-9.23%
Coupled Mode	N/A	37.82	N/A	N/A
First torsion mode (WT1)	43.80	43.06	45.44	+3.74%

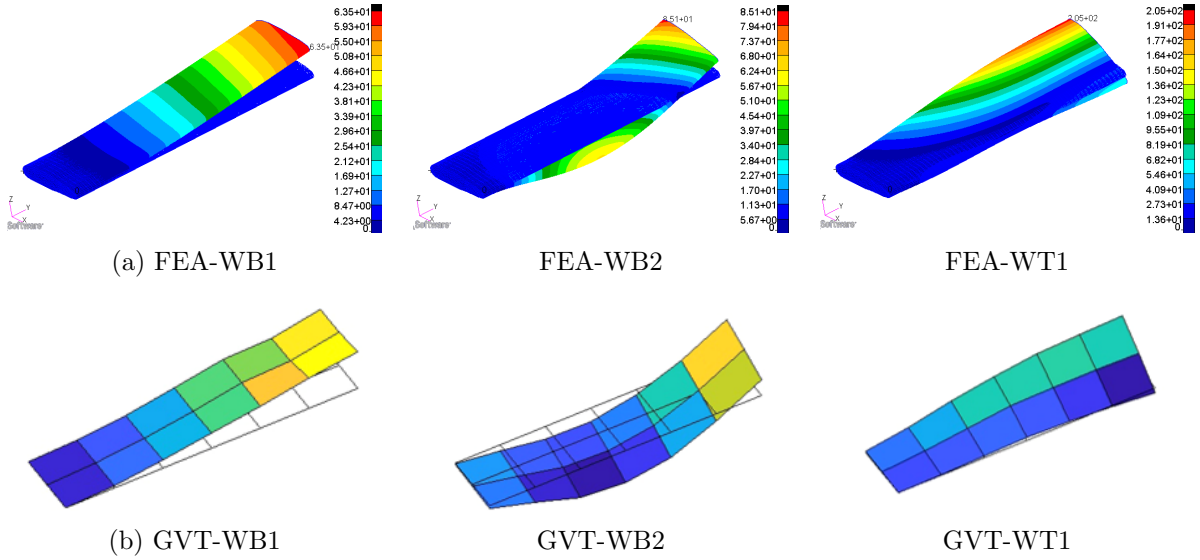

(a) FEA-WB1 FEA-WB2 FEA-WT1

(b) GVT-WB1 GVT-WB2 GVT-WT1

Figure 6: Comparison of Mode Shapes with Updated Foam Material Properties between (a) FEA Results and (b) Ground Vibration Test (GVT) Results

Comparison of ASTM Material Testing vs GVT-based Approach

A summary of the estimated material properties for the studied EPS foam model obtained from both ASTM static tests and vibration model results based FEM updating, as well as the values provided by the foam supplier, is presented in Table 3. From this, it is clear that the foam elastic modulus from the numerical estimation and ASTM material tests are in better agreement compared to the values provided by the manufacturer. Chen et al. [9] estimated the tensile Young's modulus of EPS28 and EPS13 to be 7200 kPa and 5000 kPa, which are larger than their estimate of the compressive Young's modulus of 4800 kPa and 2700 kPa. The Young's modulus that was computed using the bending static test (Approach 1) and the ground vibration test (Approach 2) fall in between the compressive and tensile moduli, as the bending mechanism involves both tension and compression.

It was observed that the shear modulus value was more sensitive to experimental uncertainties than the Young's modulus. It was postulated that the estimate from Approach 2, the GVT test, gave the shear modulus that was most representative of the loading conditions experienced during the flutter test. Also, considering the dependence of G on the specimen size [5], this approach used the same wing model that was used for flutter testing, removing any variation that was introduced due to the dimensions.

Overall, the material properties of EPS foam are dependent on the loading rate as discussed previously. These observations also highlight the importance of carrying out in-house material tests when the system dynamics are highly dependent on the material properties involved.

Table 3: Summary of Foam Material Properties from ASTM Tests and GVT-based Methods

Properties	Supplier values [4]	Model updating	ASTM C203 & C393 tests
Young's modulus, kPa	1379 (200 psi)	5274 (765 psi)	6667 (967 psi)
Shear modulus, kPa	2068 (300 psi)	2517 (365 psi)	3082 (447 psi)
Density, kg/m^3	16.3 (1.02 pcf)	12.3 (0.77 pcf)	13.1 (0.82 pcf)
Poisson's ratio	N/A	0.048	0.081

3. Flutter Testing and Prediction

This section highlights the testing procedure, together with numerical flutter analysis verification. The validity of the material model and the effect of the aerodynamic wing shape for EPS foam for this application is also verified.

3.1. Flutter Testing

Figure 7 shows the test setup of the foam wing model in the 0.7 m $\times$ 0.7 m open jet wind tunnel at Virginia Tech. The foam model fitted with a 3D printed support, similar to the GVT set-up shown in Fig. 5, was mounted on a medium density fiberboard (MDF) surface. The model was kept in place by bolting it via a hole in the MDF surface to two 80/20 aluminum extrusions, that in turn were fixed firmly to the outer frame of the wind tunnel. The model was aligned with the air flow direction along its chord-wise axis.

An ADXL335 analog accelerometer ($\pm$3g, 300 mV/g, nonlinearity $\pm$0.3% Full Scale) was employed to measure the wingtip acceleration during the tests. This approach was more suitable than using a laser vibrometer, owing to the higher rates of excitation during a flutter test and the non-smooth airfoil shape of the test model. The data was collected using a NI USB-6211 data acquisition (DAQ) system that included 16 analog input channels. The wires connecting the wingtip accelerometers to the NI DAQ were threaded through a small channel along the wing trailing edge. This minimized any interaction of these additional components with the flow. The output data and wind tunnel airspeed were logged using two separate in-house MATLAB codes. Multiple video cameras were set up to record observations for the test.

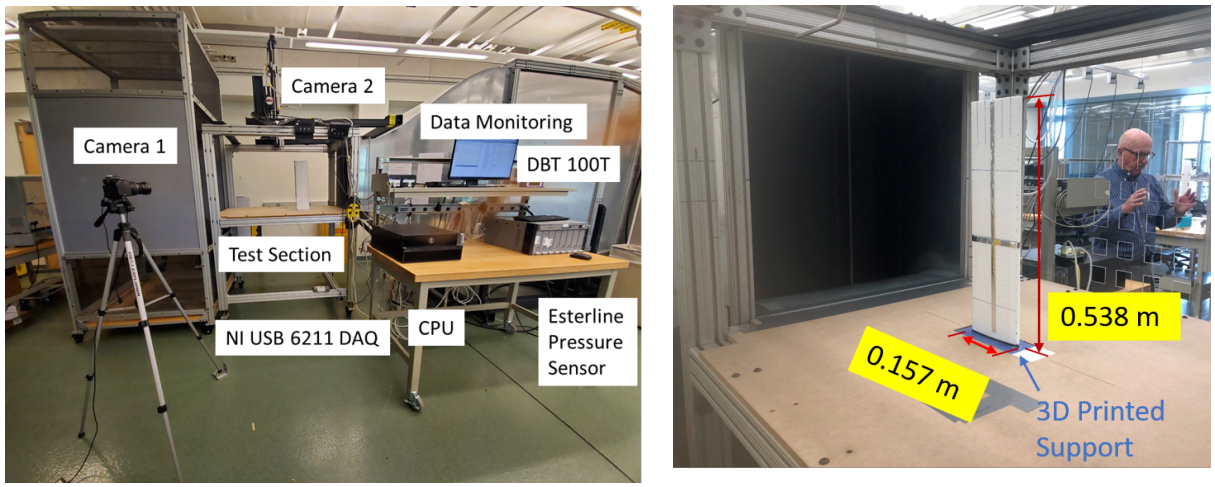

(a) Wind tunnel setup (b) Fixed foam wing model

Figure 7: Wind tunnel test setup of a clamped EPS foam wing model

3.2. Numerical Model

Since flutter is a dynamic fluid-structure interaction problem, both the structural dynamics and the aerodynamics have to be modelled to capture this phenomena. The structural dynamics model of the foam wing described in Section 2 was used here, together with low-speed, unsteady aerodynamics using the doublet-lattice method (DLM), available in the MSC NASTRAN's SOL 145 solver. Considering that the airfoil for the foam model was not smooth as is the case for the NACA 4318 airfoil itself, a corrected lift coefficient slope was used in the DLM when performing flutter analysis. The foam model had a uniform cross section across its spanwise direction. A 2D, viscous, Computational Fluid Dynamic (CFD) study was conducted for the bumpy airfoil covered with flats to obtain the lift curve in terms of various angles of attack (AoAs). A comparison of these coefficients with those for the reduced-thickness NACA 4318 airfoil are shown in Fig. 8. It was observed that the lift coefficient slope for the airfoil of the test model was lower than that for a reduced-thickness NACA 4318 airfoil, most likely due to the blunt trailing edge. So, a correction weighting factor, 0.934, was considered for the lift curve slope used in each panel of the Doublet Lattice Method (DLM) model for the foam wing. The camber effect only influences static aeroelastic

response and does not impact the flutter speed. The deformed wing shape changes under testing the aerodynamic influence coefficient matrix and the flutter speed, but that was not considered in the aerodynamic model in the present analysis as the deflections observed from the test were small. Additionally, as the present foam model has sufficient bending stiffness due to the large thickness of the foam model, geometric nonlinearity can be ignored. Therefore, a linear approach was used in studying the flutter of the EPS foam wing model.

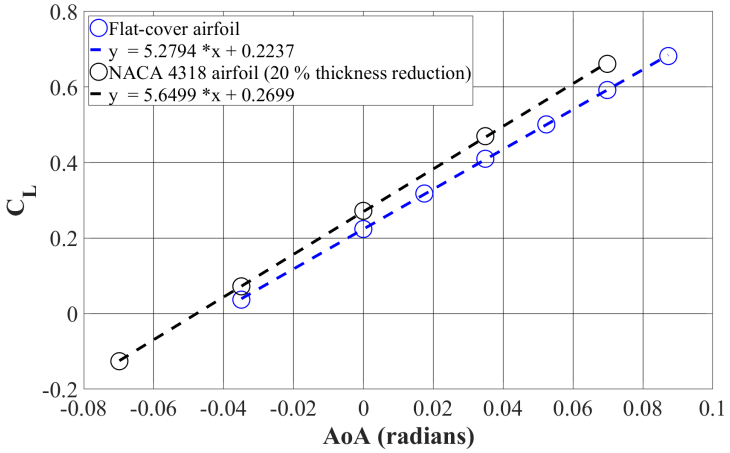

Figure 8: Lift Coefficient vs Angle of Attack for Flat-Cover Airfoil

3.3. Flutter Analysis Results

The root locus of the lowest six modes of the wing model obtained from the numerical flutter analysis in Section 3.2 are shown in Fig. 9. From this plot, it is evident that Mode 3 (the second bending mode) becomes unstable, resulting in the onset of flutter. The flutter here was in fact the result of the coupling between the second bending (Mode 1) and the first torsion modes (Mode 2) of this relatively high aspect ratio, flexible wing.

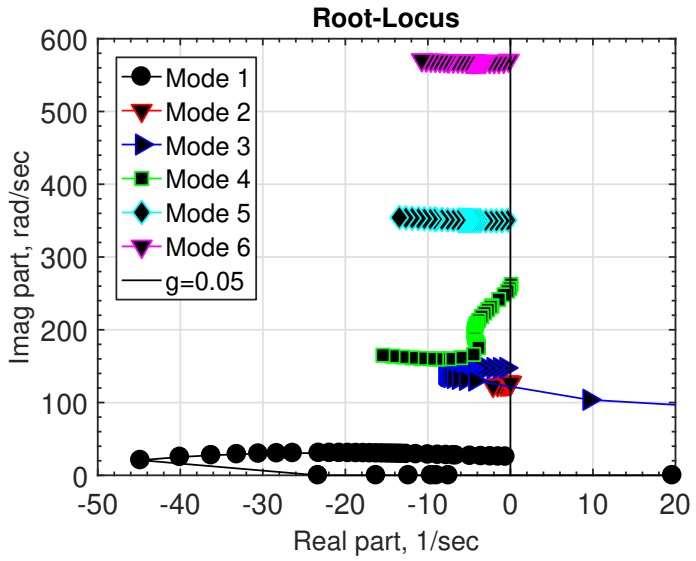

Figure 9: Root Locus of EPS Foam Wing Model

The CFDD technique was used for identifying the modal frequencies from measured time-domain acceleration from the analog accelerometers during the wind tunnel test. The raw Power Spectral Density (PSD) was passed through a low-pass filter, and an appropriate windowing function was applied. The peak picking algorithm was used to identify a peak in a specified frequency range, and then the curve fitting was performed to estimate modal parameters. The method fitted each Single-Degree-of-Freedom spectrum with a Gaussian curve. The peak picking algorithm provided the frequency data, whereas the half-power method (Butterworth, Lee, and Davidson [8]) was applied to estimate damping using Eq. (3).

$$\zeta = \frac{f_n(f_{ub} - f_{lb})}{f_{lb}^2 + f_{ub}^2} \tag{3}$$

Figure 10 shows the comparison between the damping vs airspeed relationship obtained from the flutter test and the numerical analysis. It is seen that the numerical predictions of damping in terms of air speed are in a good agreement with the test values.

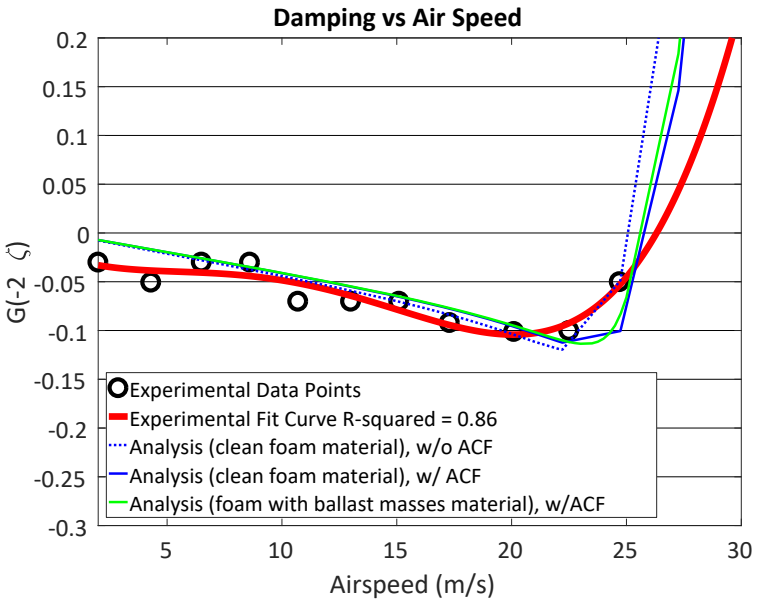

Figure 10: Comparison of damping velocity between analysis and test results

Considering a potentially large viscous damping of the present foam model, the flutter speed was computed at a higher structural damping of 5%, as summarized in Table 4. An Aerodynamic Correction Factor (ACF) was considered for the lift slope coefficient of each panel used in the DLM, unsteady aerodynamic model. It was observed that this approach led to the flutter speed prediction being close to the test data. Flutter itself was not observed during the wind tunnel test as it did not fall within the operation speed of 26 m/s of the wind tunnel. This was confirmed by the numerical prediction of the flutter speed. For practical safety reasons, the testing did not progress further up to witnessing flutter.

Table 4: Flutter Speed (m/s) of the Foam Wing Model

Structural damping, g	Experimental Test	w/o ACF	w/ ACF
g = 0	26.30	25.06	25.77
g = 5%	27.38	25.40	26.28

Finally, parametric studies were conducted to examine the impact of ACF on the flutter speed of the model. This study was performed to gather additional insights into the effect of the aerodynamic parameters on the flutter speed that would be useful in future design

efforts. In the present study, the ACF value was taken as 0.934 for all DLM aerodynamic panels. When multiplying the lift slopes of all the panels by this correction factor, there was an increase in the predicted flutter speed by around 3%, as observed in Table 4. This increase is in comparison to the case where ACF was not considered, i.e., its value is effectively 1. This tallies with the observations in Figure 11 where an increase in the flutter speed was observed when reducing the ACF parameter of all the DLM model panels. The damping values were found to be similar in lower air speeds for different ACF where the structural damping dominates.

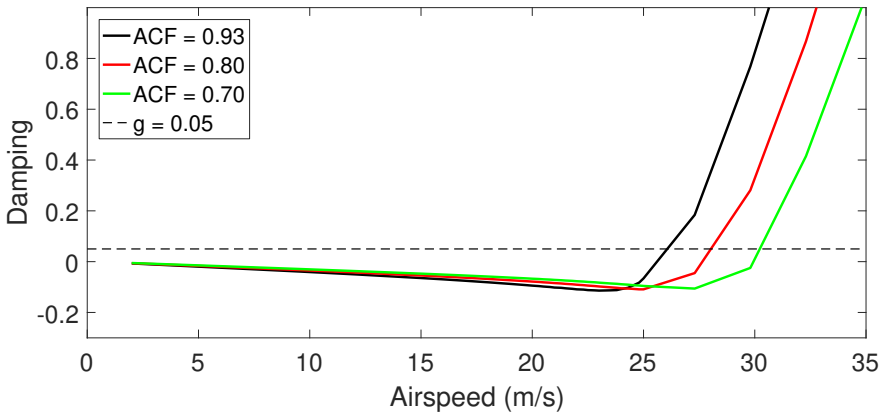

Figure 11: Damping - Airspeed plot for Different ACFs (Mode 3 is still Flutter Mode)

4. Conclusions

This work presented the analysis and experimental wind tunnel flutter testing for a low-cost expanded polystyrene foam wing model shaped after the outer mold line of an inflatable wing. The procedure and the technical challenges associated with working with this low-cost option were discussed. A novel material testing method that enabled the use of EPS foam for this purpose was developed and compared against conventional ASTM-based approaches and the general material properties provided by the manufacturer. This method involved FEM model updating based on simple ground vibration tests. It was found that GVT-based approach resulted in material properties that were more representative of the flutter testing

loads and mechanical behavior of the wing specimen. The material properties provided by the supplier and the ASTM tests, which considered the material behavior at a much lower loading rate compared to the actual flutter conditions, were different from the results obtained from the GVT-based approach.

For the unusual and non-smooth slope of the airfoil of the wing model, computational fluid dynamics results were used to correct the doublet-lattice method based aerodynamic model lift coefficient versus angle of attack slope. The aeroelastic model of the foam wing using updated material properties and corrected lift coefficient slopes in the DLM unsteady aerodynamic model, using aerodynamic correction factors, predicted the flutter results very well in agreement with the test data.

This work demonstrated a methodology that could be adopted at the preliminary stages of a more complex flutter testing effort. EPS foam was chosen for it low-cost, easy manufacturability and availability. However, as discussed, one main difficulty was the determination of accurate material properties, arising from its cellular and non-uniform nature. As the next step, the availability of other low cost options with more well-defined mechanical properties could be explored. In addition, when using foam, further testing should be done for a larger sample of specimens to investigate the sensitivity of the flutter frequency and mode shapes to the material properties.

References

[1] Aeroelastic stability substantiation of transport category airplanes: Damping requirements. Technical report, Federal Aviation Administration, 2014. URL `https://www.faa.gov/documentLibrary/media/Advisory_Circular/AC_25_629-1B.pdf`.

[2] ASTM C393/C393M-16 Core shear properties of sandwich constructions by beam flexure. ASTM Standard, ASTM International, West Conshohocken, PA, 2016.

[3] ASTM C203-05 Standard test methods for breaking load and flexural properties of block-type thermal insulation. ASTM Standard, ASTM International, West Conshohocken, PA, 2017.

[4] Polystyrene foam (EPS) data sheet, 2019. URL `https://www.foambymail.com/polystyrene-foam-sheet.html`. [Accessed: November 2019].

[5] Sigitas AVėjelis, Ivan Gnip, Saulius Vaitkus, and Vladislovas Keršulis. Shear strength and modulus of elasticity of expanded polystyrene (eps). *Material Science (MEDŽIAGOTYRA)*, 14(3), 2008. ISSN 1392–1320.

[6] Raymond L. Bisplinghoff and Holt Ashley. *Principles of Aeroelasticity, Reissued Version*. Dover Publications, Inc., Mineola, New York, 2013.

[7] Christopher E. Brennen. *An Internet Book on Fluid Dynamics: Values of the Added Mass*. 2006. URL `http://brennen.caltech.edu/fluidbook/basicfluiddynamics/unsteadyflows/addedmass/valuesoftheaddedmass.pdf`. [Accessed: June-04-2020].

[8] John Butterworth, Jin Hee Lee, and Barry Davidson. Experimental determination of modal damping from full scale testing. In 13^{th} *World Conference on Earthquake Engineering, Vancouver*, volume 310, pages 1–15, 2004.

[9] Wensu Chen, Hong Hao, Dylan Hughes, Yanchao Shi, Jian Cui, and Zhong-Xian Li. Static and dynamic mechanical properties of expanded polystyrene. *Materials & Design*, 69:170–180, 2015.

[10] William Gracey. The additional-mass effect of plates as determined by experiments. *NASA Technical Report*, 1942. Report No. 707.

[11] Abhineet Gupta, Peter J. Seiler, and Brian P. Danowsky. Ground vibration tests on a

flexible flying wing aircraft-invited. In *AIAA Atmospheric Flight Mechanics Conference*, San Diego, California, USA, 2016. doi: 10.2514/6.2016-1753.

[12] Dewey H. Hodges and G. Alvin Pierce. *Introduction to Structural Dynamics and Aeroelasticity, Second Edition*. Cambridge University Press, 2011. page. 182, New York.

[13] Rick Lind. Flight-test evaluation of flutter prediction methods. *Journal of Aircraft*, 40 (5):964–970, 2003. doi: 10.2514/2.6881.

[14] Attapole Malai and Sompote Youwai. Stiffness of expanded polystyrene foam for different stress states. *International Journal of Geosynthetics and Ground Engineering*, 7 (4), 2021. doi: 10.1007/s40891-021-00321-7.

[15] Jitish Miglani, Wei Zhao, Siddhant Desai, Varakini Sanmugadas, Joseph A Schetz, and Rakesh K Kapania. Analysis, design, and experiments of metal flat plate and foam airfoil flutter test articles. In *AIAA Scitech 2021 Forum*, 2021. doi: 10.2514/6.2021-1497.

[16] Simon Ouellet, Duane Cronin, and Michael Worswick. Compressive response of polymeric foams under quasi-static, medium and high strain rate conditions. *Polymer Testing*, 25(6):731–743, 2006. doi: https://doi.org/10.1016/j.polymertesting.2006.05.005.

[17] Umud Esat Ozturk and Gunay Anlas. Finite element analysis of expanded polystyrene foam under multiple compressive loading and unloading. *Materials & Design*, 32(2): 773–780, 2011. doi: 10.1016/j.matdes.2010.07.025.

[18] Shardul S. Panwar, Rikin Gupta, Azwan Aris, Taewoo Nam, Jitish Miglani, Wei Zhao, and Rakesh K. Kapania. In *3D-Photogrammetric Modal Testing and Data Analysis of a Cantilevered Inflatable Wing*, 2022. doi: 10.2514/6.2022-1513.

[19] Harald Pfifer and Brian P Danowsky. System identification of a small flexible aircraft-

invited. In *AIAA Atmospheric Flight Mechanics Conference*, San Diego, California, USA, 2016. doi: 10.2514/6.2016-1750.

[20] Alejandro E Rodríguez-Sánchez and Héctor Plascencia-Mora. A machine learning approach to estimate the strain energy absorption in expanded polystyrene foams. *Journal of Cellular Plastics*, 58(3):399–427, 2022. doi: 10.1177/0021955X211021014.

[21] Josefine Severholt. Generic 6-dof added mass formulation for arbitrary underwater vehicles based on existing semi-empirical methods. Master's thesis, Royal Institue of Technology, 2017.

[22] Stuart J Shelley and Charles R Pickrel. New concepts for flight flutter parameter estimation. In *Proceedings-SPIE The International Society for Optical Engineering*, pages 490–496, 1997.

[23] Jie Zeng and Sunil L Kukreja. Flutter prediction for flight/wind-tunnel flutter test under atmospheric turbulence excitation. *Journal of Aircraft*, 50(6):1696–1709, 2013. doi: 10.2514/1.C031710.

[24] Wei Zhao, Abhineet Gupta, Christopher D Regan, Jitish Miglani, Rakesh K Kapania, and Peter J Seiler. Component data assisted finite element model updating of composite flying-wing aircraft using multi-level optimization. *Aerospace Science and Technology*, 95:105486, 2019. doi: 10.1016/j.ast.2019.105486.

[25] Wei Zhao, Siddhant Desai, Jitish Miglani, Rakesh K. Kapania, Joseph A. Schetz, Azwan Aris, and Shardul Panwar. Structural and aeroelastic design, analysis, and experiments of inflatable airborne wings. In *AIAA SciTech 2021 Forum*, Virtual Meeting, 2021. doi: 10.2514/6.2021-1817.